Available online at www.sciencedirect.com
ScienceDirect
Bioorganic & Medicinal Chemistry 15 (2007) 6109–6118
Bioorganic & Medicinal Chemistry

'Bridged' stilbene derivatives as selective cyclooxygenase-1 inhibitors

Norbert Handler,[a] Gerda Brunhofer,[a] Christian Studenik,[b] Klaus Leisser,[a] Walter Jaeger,[c] Stephanie Parth[a] and Thomas Erker[a,*]

[a]*Department of Medicinal Chemistry, University of Vienna, Althanstrasse 14, A-1090 Vienna, Austria*
[b]*Department of Pharmacology and Toxicology, University of Vienna, Althanstrasse 14, A-1090 Vienna, Austria*
[c]*Department of Clinical Pharmacy and Diagnostic, University of Vienna, Althanstrasse 14, A-1090 Vienna, Austria*

Received 11 September 2006; revised 8 June 2007; accepted 15 June 2007
Available online 20 June 2007

Abstract—Resveratrol ((*E*)-3,4′,5-trihydroxy-stilbene), a phytoalexin found in various plants, shows non-selective cyclooxygenase-1 (COX-1) and cyclooxygenase-2 (COX-2) inhibition. In order to find more selective COX inhibitors a series of bridged stilbene derivatives was synthesized and evaluated for their ability to inhibit both COX-1 and COX-2 in vitro. The compounds showed a high rate of COX-1 inhibition with the most potent compounds exhibiting submicromolar IC_{50} values and high selectivity indices. A prediction model for COX-inhibiting activity was also developed using the classical LIE approach resulting in consistent docking data for our molecule sample. Phenyl substituted 1,2-dihydronaphthalene derivatives and 1*H*-indene derivatives therefore represent a novel class of highly selective COX-1 inhibitors and land promising candidates for in vivo studies.

1. Introduction

Resveratrol ((*E*)-3,4′,5-trihydroxy-stilbene) is a phytoalexin found in various plants, especially in the skin of grapes and in consequence also in red wine. This stilbene derivative demonstrates anti-inflammatory, cardiovascular protective, and cancer chemopreventive properties.[1] Resveratrol has been reported to play a role in the prevention of heart diseases associated with red wine consumption because it inhibits platelet aggregation,[2] alters eicosanoid synthesis,[2,3] and modulates lipid and lipoprotein metabolism.[4,5] Further it was found to be a non-selective inhibitor of COX-1 and COX-2.[6]

The enzymes COX-1 and COX-2 catalyze the first two steps in the synthesis of all vasoactive prostaglandins (PGs). Two distinct active sites on these enzymes are responsible for the conversion of arachidonic acid to PGH_2.[7–9] This bicyclic peroxide is the starting compound in the biosynthesis of other PGs and thromboxanes (Tx). Among others, PGs are mediators of the vascular homeostasis. Though, thromboxane TxA_2 acts as a potent vasoconstrictor and platelet aggregator and it is synthesized in activated platelets by COX-1. In contrast, PGI_2 is a potent vasodilator and an antiplatelet aggregator and is synthesized in the vascular endothelial cells by COX-2.[9–11] Selective inhibition of COX-1 offers an opportunity for developing a new class of cardioprotective agents by tilting the TxA_2-PGI_2 balance in favor of PGI_2, a way, that low-dose aspirin exerts its cardioprotective effects.[12–15]

Furthermore, experimental and clinical results have suggested a possible involvement of COX-1 in cancer and pain development.[16–20] In fact, epidemiological data showed that regular use of low-dose aspirin, which inhibits selective platelet COX-1 activity, can reduce colon cancer incidence and mortality.[21–23] Thus, selective COX-1 inhibitors might be useful cardioprotective, chemopreventive, and analgesic agents.

Concerning the serious gastrointestinal adverse effects of non-selective NSAIDs, the following matter of fact could be stated: selective COX-2 inhibitors as well as selective COX-1 inhibitors are more efficacious as non-selective NSAIDs for the therapy of different diseases. Both selective inhibitors show the advantage of reduced gastrointestinal toxicity associated with the administration of non-selective NSAIDs.[24]

Keywords: COX-inhibition; Resveratrol; COX-1; Stilbene; Docking model.
* Corresponding author. Tel.: +43 1 4277 55003; fax: +43 1 4277 9551; e-mail: thomas.erker@univie.ac.at

0968-0896/$ - see front matter © 2007 Elsevier Ltd. All rights reserved.
doi:10.1016/j.bmc.2007.06.030

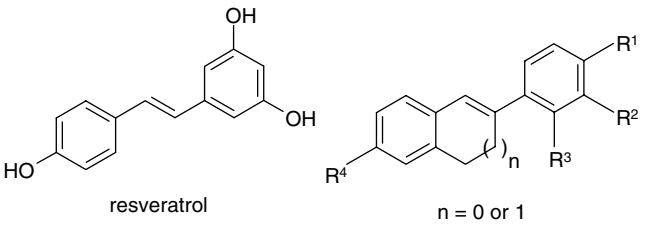

Figure 1. General structure of "bridged" stilbene derivatives.

The simplicity of resveratrol, associated with its interesting biological activities, offers pathways for rational design of new therapeutic agents, and in this context, recent efforts have been devoted to the detailed study of structure–activity relationships (SAR) of this type of substituted stilbene derivatives.[25–27] In this paper, we want to present the synthesis of novel stilbene derivatives and their influence on the COX-1/COX-2 system.

As demonstrated before, some hydroxylated or methoxylated resveratrol analogues exhibited a several fold higher COX-2 selectivity than resveratrol[28] and in continuation we investigated in this paper whether bridged resveratrol analogues might favor a better and more selective COX-1 inhibition than resveratrol.

As part of our ongoing program to design novel selective COX-1 inhibitors, we present herein the synthesis and biological evaluation of a new class of stilbenes bridged by a methylene or ethylene group or usually named 1,2-dihydronaphthalene derivatives and 1*H*-indene derivatives as shown in Figure 1.

Five dihydronaphthalene derivatives and three 1*H*-indene derivatives were therefore synthesized using standard chemical methods. Each analogue was then tested for COX-1 and COX-2 inhibition in an in vitro model and the resulting inhibition values were compared with that of resveratrol, with the clinically established selective COX-2 inhibitor celecoxib and with aspirin. In addition, as resveratrol exerts vasodilating effects on blood vessels,[29] selected compounds were investigated for their relaxing effect on smooth muscles. Structure–activity

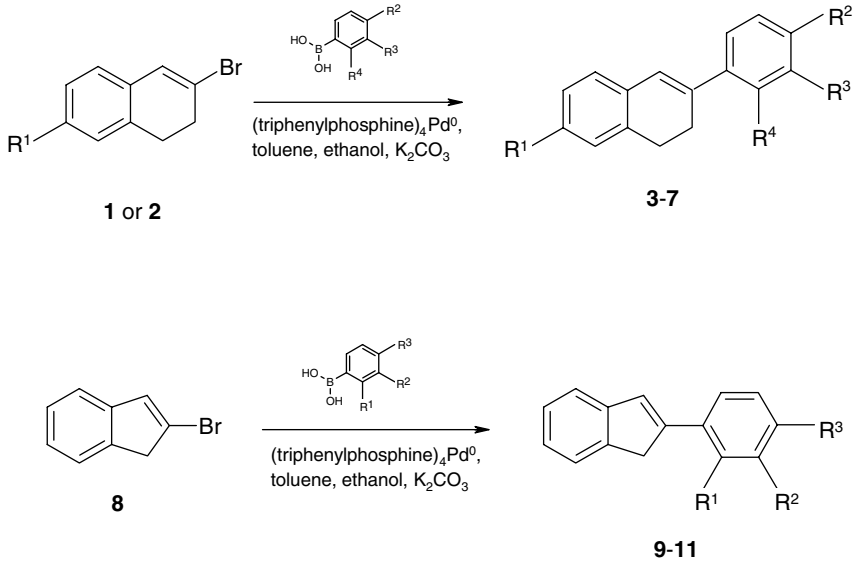

Compound	^{1}R	^{2}R	^{3}R	^{4}R
1	-H	--	--	--
2	-OCH_3	--	--	--
3	-H	-OCH_3	-OCH_3	-OCH_3
4	-H	-OCH_3	-OCH_3	-H
5	-H	-O-CH_2-O-		-H
6	-OCH_3	-OCH_3	-OCH_3	
7	-OCH_3	-OCH_3	-OCH_3	-OCH_3
8	-H	--	--	--
9	-H	-O-CH_2-O-		--
10	-OCH_3	-H	-H	--
11	-OCH_3	-OCH_3	-OCH_3	--

Scheme 1. Synthesis and chemical structures of provided compounds.

relationship (SAR) studies were conducted to evaluate the effects of various structural parameters of the molecules on COX-1 and COX-2 inhibition.

2. Results and discussion

2.1. Chemistry

The 1,2-dihydronaphthalene derivatives (**3**–**7**) and 1*H*-indene derivatives (**9**–**11**) were synthesized using standard chemical methodologies (resveratrol was obtained from a commercial supplier and was of analytical grade) (Scheme 1).

The corresponding phenyl substituted 1,2-dihydronaphthalene derivatives were obtained from 3-bromo-1,2-dihydronaphthalene (**1**)[46] via Suzuki reaction with the appropriate phenylboronic acid derivative. Compound **1** was synthesized starting with the bromination of 1-tetralone with bromine, reduction with $NaBH_4$, and elimination of H_2O. The following Suzuki coupling reactions with the substituted boronic acids were carried out at 90 °C in the presence of potassium carbonate and tetrakis(triphenylphosphine)palladium(0) as catalyst to afford the desired methoxy compounds **3**–**7** in good yields. The corresponding phenyl substituted 1*H*-indene derivatives were synthesized in the same manner starting from 1-indanone to yield 2-bromo-1*H*-indene[47] and finally molecules **9**–**11** smoothly.

2.2. Inhibition of COX-1 and COX-2

Inhibition of COX-1 and COX-2 by the compounds described above was analyzed in a cell-free immunoassay system. Purified ovine enzyme served as the source of COX-1, while the human recombinant enzyme formed the source of COX-2. The inhibition of COX-1 and COX-2 is shown in Table 1 with IC_{50} values given in μM and corresponding selectivity indices compared to resveratrol, celecoxib and aspirin.

Table 1. Inhibitory effect of **3**–**7**, **9**–**11** and the reference compounds resveratrol, celecoxib, and aspirin on COX-1 and COX-2 activity

Compound	IC_{50} (COX-1) (μM)	IC_{50} (COX-2) (μM)	Selectivity index COX-2/COX-1
3	0.48	0.66	1.38
4	61.1	>100	>1.63
5	>100	>100	—
6	0.38	0.03	0.079
7	0.015	>100	>6666
9	12.8	>100	>7.8
10	0.46	62.3	135
11	0.03	1.33	44.3
Resveratrol	0.535	0.996	1.86
Celecoxib	19.03	0.035	0.0018
Aspirin	90–100	100–110	1

The data presented herein pointed out that aspirin was a weak, non-selective inhibitor of both isoenzymes (IC_{50} for COX-1 and COX-2 about 100 μM), whereas reseveratrol possessed micromolar, non-selective inhibitory action (IC_{50} for COX-1 and COX-2 about 1 μM). On the other hand, celecoxib showed potent and selective COX-2 inhibition (IC_{50}(COX-2) = 0.035 μM).

Concerning our molecules, a clear SAR could be achieved, since only polymethoxylated molecules exhibited selective and potent COX-1 inhibition. The dioxolane derivatives **5** and **9** possessed no relevant inhibitory effects on both isoenzymes with IC_{50} values from 12.5 and 63 μM to >100 μM. In contrast, the methoxy derivatives, especially compounds **7** and **11**, were potent inhibitors of COX-1 exhibiting IC_{50} values of 0.015 μM for **7** and 0.03 μM for **11**, respectively. In general, the inhibitory effect toward COX-1 could be improved by adding an increasing number of methoxy-groups as shown for both 1,2-dihydronaphthalene and 1*H*-indene. Thus, compound **7** exhibited a 10-fold higher inhibitory action than molecule **6** (IC_{50} (COX-1) = 0.015 μM vs 0.38 μM) and the same trend could be observed for the 1-*H*-indene derivatives **11** and **10** (IC_{50}(COX-1) = 0.03 μM vs 0.46 μM).

Based on the IC_{50} values for COX-1 and COX-2, the relative ratios of IC_{50} COX-2/ IC_{50} COX-1 were calculated and the data are also presented in Table 1. The selectivity indices for the novel compounds ranged from 0.079 (compound **6**) representing a COX-2-selective molecule and 135 (compound **10**) representing a COX-1-selective molecule to a ratio of >6666 for compound **7**, hence showing no affinity toward COX-2.

2.3. Effects on smooth muscles

The effects of the compounds **3**, **4**, **9**, **10**, and **11** on terminal ilea, aortic, and arteria pulmonalis rings were investigated in concentrations between 0.3 and 100 μmol/L (Table 2). Compound **3** did not change force of contraction (f_c) in terminal ilea ($n = 3$, 100 μmol/L) and in aortic ($n = 3$, 100 μmol/L) but slightly reduced f_c in arteria pulmonalis rings to −11.01 ± 6.72% ($n = 3$,

Table 2. Relaxing effect of resveratrol and selected compounds **2**, **6**, **7**, and **8** on smooth muscle preparations

Compound	Terminal ileum (decrease of f_c at 100 μM, $n = 3$)	Aorta rings (decrease of f_c at 100 μM, $n = 3$)	Arteria pulm. rings (decrease of f_c at 100 μM, $n = 3$)
4	−45.34 ± 10%	−15.97 ± 14%	−41.45 ± 9%
9	−51.74 ± 7%	−28.08 ± 2%	−19.82 ± 3%
10	−40.89 ± 12%	−35.72 ± 2%	−26.08 ± 3%
11	−35.94 ± 14%	−3.45 ± 10%	−11.92 ± 11%
Resveratrol	−64.77 ± 2% ($n = 5$)	−55.15 ± 7% ($n = 5$)	−53.56 ± 7% ($n = 5$)

100 μmol/L). Compound **4** exerted a more potent effect. Reduction of f_c in terminal ilea was $-45.34 \pm 10.80\%$ ($n = 3$, 100 μmol/L), in aortic rings $-15.97 \pm 14.61\%$ ($n = 3$, 100 μmol/L), and in arteria pulmonalis rings $-41.45 \pm 9.36\%$ ($n = 3$, 100 μmol/L). Compound **9** decreased f_c in terminal ilea to $-51.74 \pm 7.93\%$ ($n = 3$, 100 μmol/L), in aortic rings to $-28.08 \pm 1.71\%$ ($n = 3$, 100 μmol/L), and in arteria pulmonalis rings to $-19.82 \pm 3.59\%$ ($n = 3$, 100 μmol/L). Compound **10** showed similar effects with a reduction of f_c in terminal ilea to $-40.89 \pm 11.90\%$ ($n = 3$, 100 μmol/L), in aortic rings to $-35.7 \pm 2.54\%$ ($n = 3$, 100 μmol/L), and in arteria pulmonalis rings to $-26.08 \pm 3.58\%$ ($n = 3$, 100 μmol/L). Compound **11** was less effective. It lowered f_c in terminal ilea to $-35.94 \pm 14.29\%$ ($n = 3$, 100 μmol/L), in aortic rings to $-3.45 \pm 10.61\%$ ($n = 3$, 100 μmol/L), and in arteria pulmonalis rings to $-11.92 \pm 11.17\%$ ($n = 3$, 100 μmol/L).

All compounds studied did not show a significant vasodilatory effect which has been reported for resveratrol before, indicating that there is no difference between compounds with an 1*H*-indene moiety or a 1,2-dihydronaphthalene moiety.

2.4. Docking simulation

2.4.1. Theoretical methods. Rigorous computational methods such as FEP (free energy perturbation) have shown to predict experimental binding affinities of COX-1 and COX-2 well.[30,31] FEP is able to predict accurate relative free energies of binding but is limited in the number of inhibitor–protein complexes investigated due to the high computational demands. As a compromise between accuracy and computational speed, Aquist and Marelius[32] have developed the linear interaction energy (LIE) approach, which has been applied to many systems with very good results (in the order of 1 kcal/mol). Underlying this method is the assumption, that the free energy of binding can be modeled by the two endpoints of the thermodynamic cycle of ligand binding. These endpoints are the free ligand solvated and the bound ligand solvated. For these two models simulations are carried out. Aquist and Marelius used molecular dynamic simulations to obtain ensemble averages (denoted by $\langle\ \rangle$) of the intermolecular van der Waals (vdw) and electrostatic (elec) interactions. The binding free energy of interaction was then derived by the following formula:

$$\Delta G_{\text{bind}} = \alpha\langle\Delta U_{\text{vdw}}\rangle + 0.5\langle\Delta U_{\text{elec}}\rangle \quad \text{Formula 1}$$

The Δ term indicates the energy difference between ligand bound and free states. The van der Waals term is included to account for the non-electrostatic contributions to the free energy of binding. The non-polar terms are assumed to be correlated to the van der Waals interactions. As a result the parameter α is added, which can be adjusted by linear regression using experimental data.

In later publications, Aquist proposed an adjustable β parameter based on charges and number of hydroxyl groups.

Other groups proposed a third parameter to fit to experimental data. Carlson and Jorgensen proposed the introduction of the Solvent Accessible Surface Area as a third parameter.[33] The formula results to:

$$\Delta G_{\text{bind}} = \alpha\langle\Delta U_{\text{vdw}}\rangle + \beta\langle\Delta U_{\text{elec}}\rangle + \gamma\langle\Delta\text{SASA}\rangle \quad \text{Formula 2}$$

ΔSASA represents the change in the solvent accessible surface area. Other variants of the LIE methodology have also been published.[34] The inclusion of the SASA term was rationalized as accounting for the cost of cavitations and allowing for positive free energies of hydration.

In this paper, we performed LIE calculation for a series of eight COX-1/COX-2 inhibitors. We tried to show the reason for substrate specificity of the inhibitors under investigation.

2.4.2. Docking. Docking simulations were carried out using package Autodock 3.0.5[35] and DOCK 5.4.[36,37]

Ligands were modeled using program MOE and energy minimized with MMF94x force field as implemented by MOE (Chemical Computing Group, 1010 Sherbrooke Street West, Suite 910, Montreal, Quebec, H3A 2R, Canada) and a dielectric constant of 1.5. We performed a full conformational search on each of the ligands and retained only conformers having an energy difference of not more than 5 kcal/mol regarding the found global minimum conformation and a RMSD (root mean square distance of all atoms of the conformer in regard to all other conformers in the database) value greater than 0.1 Å. The charges for each conformer were derived by fitting to an electrostatic potential surface from a quantum mechanical calculation at a 6-31G*(2d,2p) level of theory with GAMESS.[38,39] Every conformation of a ligand was used in turn as a starting point for a docking run with AutoDock 3.0 and DOCK 5.4, respectively.

We used the Lamarckian Genetic Algorithm global optimizer and the Solis and Wets local optimizer as implemented in AutoDock 3. for the subsequent docking runs with Autodock 3.0.[40]

With the DOCK 5.4 package we used the default values for ligand flexibility and ligand scoring.

The best docking results from each run were taken as the starting conformations for the subsequent molecular dynamics study (Tables 3 and 4).

Figures 2 and 3 show the docked conformers of compound **7** to COX-1 and COX-2, respectively. Compound **7** exhibits a hydrogen bond to SER 530 of COX-1 whereas it does not form a hydrogen bond to COX-2. It is our hypothesis that this is one of the reasons for the COX-1 selectivity of **7**. As this cannot be the only reason we tried to correlate the binding of all compounds to the calculated linear interaction energies.

Table 3. Results of docking with COX-1

Compound	ΔU_{elec} (kJ mol^{-1})	ΔU_{LJ} (kJ mol^{-1})	ΔG(COX-1) (kJ mol^{-1})
3	−5.408	−77.042	−35.68
4	−2.231	−74.176	−23.79
5	7.188	−64.333	<−22.59
6	−9.456	−80.721	−36.25
7	−11.818	−83.208	−44.10
9	−7.406	−68.446	−27.63
10	−1.950	−78.737	−35.78
11	−7.988	−80.595	−42.48

Table 4. Results of docking with COX-2

Compound	ΔU_{elec} (kJ mol^{-1})	ΔU_{LJ} (kJ mol^{-1})	ΔG(COX-2) (kJ mol^{-1})
3	−3.563	−78.206	−34.91
4	−1.754	−76.349	<−22.59
5	−1.702	−75.161	<−22.59
6	−2.567	−87.202	−42.29
7	−0.628	−78.681	<−22.59
9	−0.436	−75.686	<−22.59
10	−1.595	−79.138	−23.75
11	−2.790	−83.338	−33.19

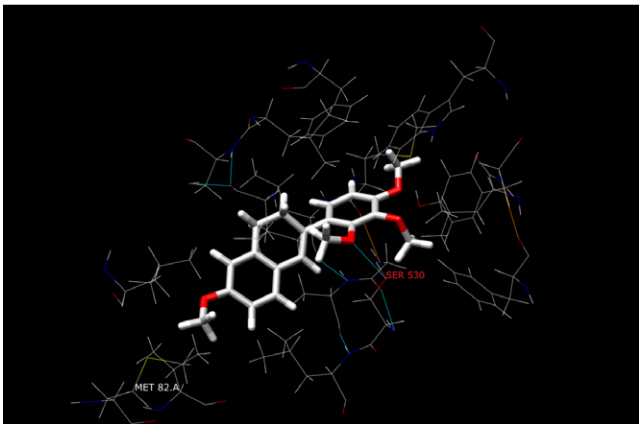

Figure 2. Compound **7** docked to COX-1.

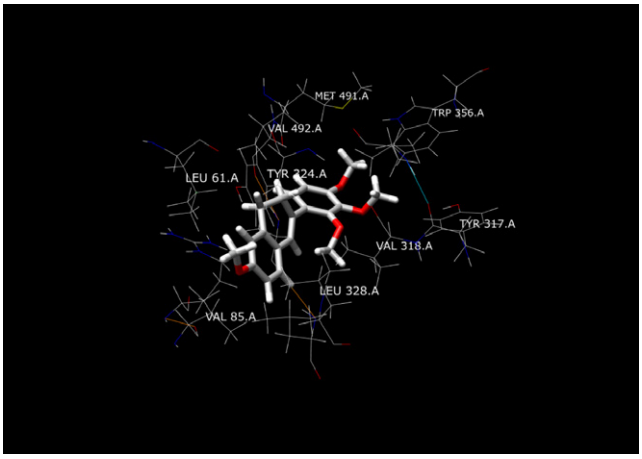

Figure 3. Compound **7** docked to COX-2.

2.4.3. Molecular dynamics. Average LIE Energies were derived by molecular dynamics simulation using program GROMACS 3.0[41] with the GROMACS force field. Input topology files of ligand structures for GROMACS were generated with PRODRUG.[42] Charges were fitted to the electrostatic potential calculated at a B3LYP/6-31G* level of theory with GAMESS.

Input topologies of the macromolecules were prepared from the structures used for docking with pdb2gmx as provided by the GROMACS package. Histidine residues were modeled as protonated states. This resulted in a overall charge of +6. This charge was neutralized by adding 6 chloride ions. The SPC water model[43] was used as solvent. The solvent box was chosen to be a octahedral periodic box with the box edges 10 Å away from the drug receptor complex.

Each drug receptor complex was energy minimized with the GROMACS force field to a maximum force of 2000 kJ mol^{-1} nm^{-1} using a steepest decent algorithm.

Subsequently we performed a dynamics simulation for 50 ps with a time step of 0.0025 ps leaving the position of the protein immobile and only ligand molecule and solvent molecules flexible.

After this simulation we carried out a 250 ps NVT molecular dynamics simulation using a time step of 0.002 ps. The NVT ensemble (canonical ensemble) keeps the number of moles, the volume, and the temperature via the Berendsen algorithm fixed. The conformations and energy values were sampled every 0.01 ps. Only conformations and energies between 100 and 150 ps were stored in order to sample only trajectories at equilibrium state. The non-bonded cutoff was chosen to be 10 Å. Figures 4 and 5 show the electrostatic and Lennard–Jones interaction energy of compound **4** solvated and complexed with COX-1. Figures 6 and 7 depict the electrostatic and Lennard–Jones interaction energy of solvated, uncomplexed compound **4** with SPC216 water.

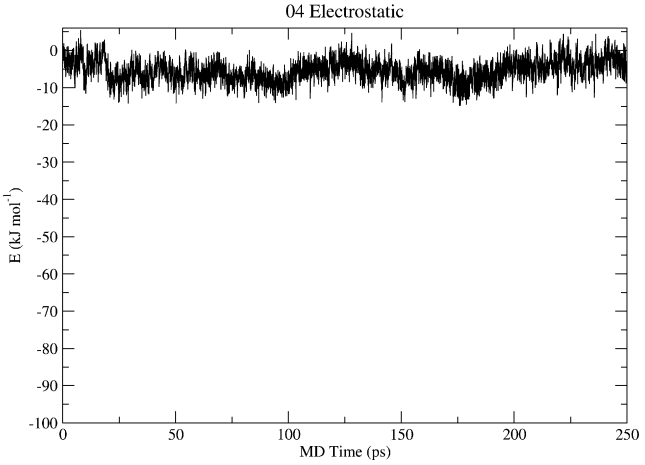

Figure 4. Electrostatic interaction energy of **4** with COX-1.

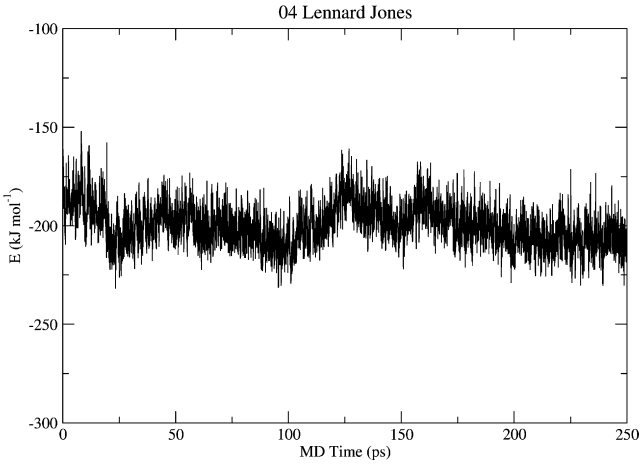

Figure 5. Lennard–Jones interaction energy of **4** with COX-1.

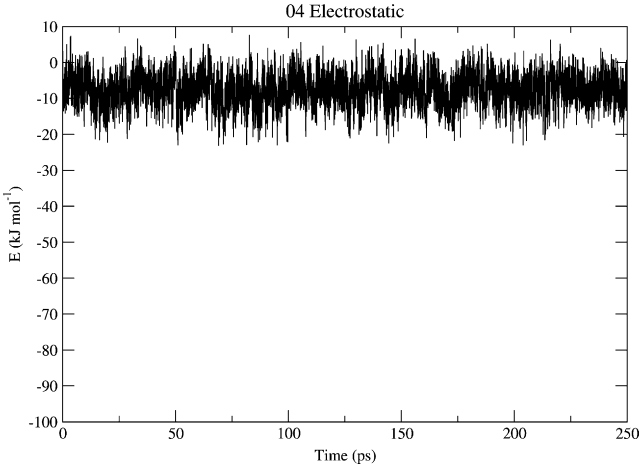

Figure 6. Electrostatic interaction energy of **4** with SPC216 water (solvent).

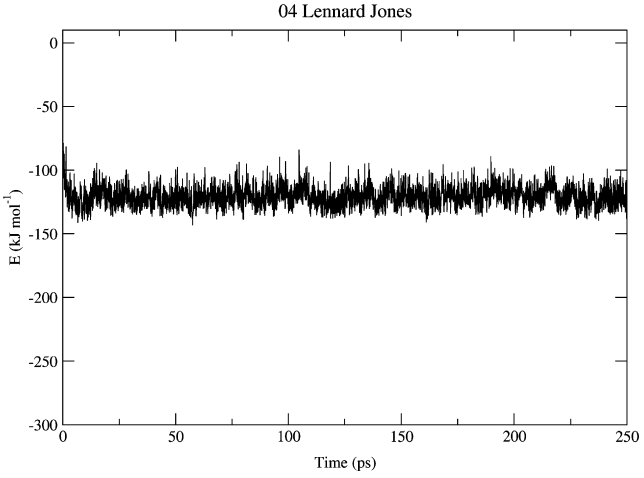

Figure 7. Lennard–Jones interaction energy of **4** with SPC216 water (solvent).

As published by Tounge and Reynolds,[44] especially the electrostatic term of the LIE equation is very susceptible to different computational preparation methods of the protein and the choice of the non-bonded cutoff. We decided to choose a 10 Å non-bonbed cutoff.

We decided to use the classical two-parameter LIE equation using ΔU_{elec} and ΔU_{LJ} because the number of compounds to study is rather small and the cross-validated r^2 (q^2) indicated a better prediction ability of the two-parameter model in both COX-1 and COX-2 results. Furthermore, the *F*-value of the ΔSASA (Solvent Accessible Surface Area) in the regression analysis was not statistically significant.

All statistical analyses were done with SPSS 10.0 (Windows) and Leave-one-out cross-validation was performed with MOE (Chemical Computing Group, 1010 Sherbrooke Street West, Suite 910, Montreal, Quebec, H3A 2R, Canada). Figures 8 and 9 show the fitting of

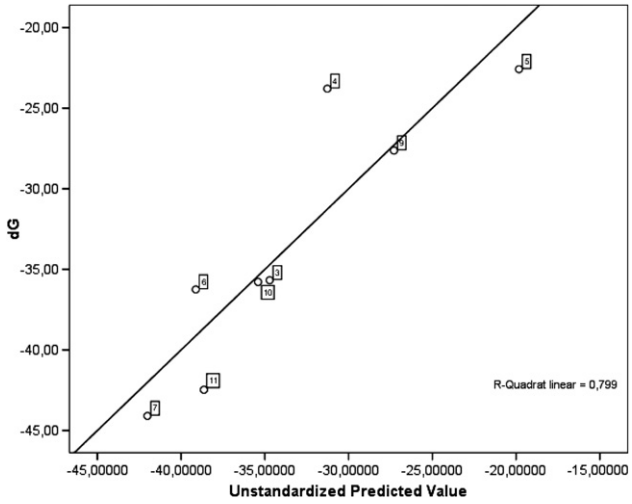

Figure 8. COX-1 regression.

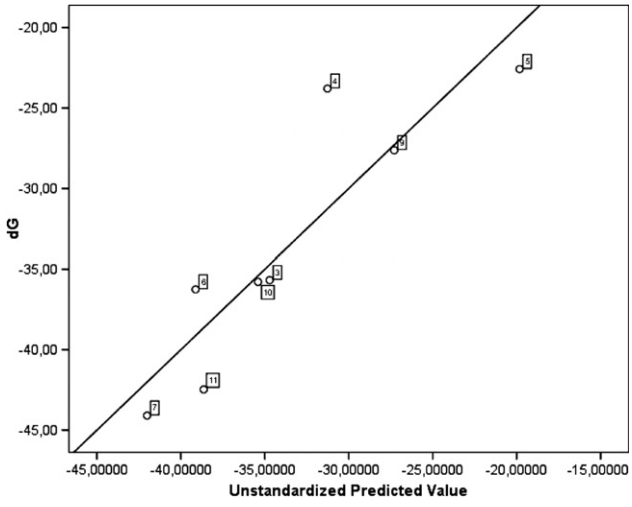

Figure 9. COX-2 regression.

the experimental values by the obtained regression equations.

The best regression equation obtained for COX-1 was

$$\Delta G_{calc} = 0.251\langle \Delta E_{elec} \rangle + 0.922\langle \Delta E_{LJ} \rangle + 37.703$$

yielding a correlation coefficient r^2 of 0.80 and a RMSE (root mean square error) of 3.39.

The best regression equation for COX-2 was

$$\Delta G_{calc} = 3.370\langle \Delta E_{elec} \rangle + 1.186\langle \Delta E_{LJ} \rangle + 72.191$$

yielding a correlation coefficient r^2 of 0.89 and a RMSE (root mean square error) of 2.43.

The Leave-one-out cross-validation procedure yielded for COX-1 a cross-validated r^2 (q^2) of 0.64 and a cross-validated RMSE of 5.50.

The Leave-one-out cross-validation procedure yielded for COX-2 a cross-validated r^2 (q^2) of 0.59 and a cross-validated RMSE of 4.78.

These results show a good fit of both the COX-1 and COX-2 model to the measured biological data and a reasonable predictivity of the model.

The slightly lower predictivity of the COX-2 model might be due to an underrepresentation of biologically active compounds and the few overall number of tested and studied compounds.

Due to the small number of conformers and the structural similarity of the compounds the predictive value of the model is limited.

3. Conclusions

In summary, we have demonstrated that bridged stilbene derivatives especially compounds **7** and **11** were selective COX-1 inhibitors with only poor COX-2 affinity. This should result in lower doses necessary to achieve a good efficacy for COX-1 inhibitors in clinical studies. Compared to resveratrol the selected compounds had no or just moderate effects on terminal ilea and vascular smooth muscle. Additionally, a prediction model for inhibitors of COX-1 and COX-2 was developed using the classical LIE approach. The model was able to discriminate between COX-1 and COX-2 inhibition and reproduced the trends in experimental activity in a series of bridged stilbene derivatives well.

4. Experimental

4.1. Cyclooxygenase assay

The effect of the test compound on COX-1 and COX-2 was determined by measuring prostaglandin E_2 (PGE_2) using a COX Inhibitor Screening Kit (Catalog No. 560131) from Cayman Chemicals, Ann Arbor, Michigan, USA. Reaction mixtures were prepared in 100 mM Tris–HCl buffer, pH 8.0, containing 1 μM heme and COX-1 (ovine) or COX-2 (human recombinant) and preincubated for 10 min in a waterbath (37 °C). The reaction was initiated by the addition of 10 μL arachidonic acid (final concentration in reaction mixture 100 μM). After 2 min the reaction was terminated by adding 1 M HCl and PGE_2 was quantitated by an ELISA method. The test compounds were dissolved in DMSO and diluted to the desired concentration with 100 mM potassium phosphate buffer (pH 7.4). Following transfer to a 96-well plates coated with a mouse anti-rabbit IgG, the tracer prostaglandin acetylcholine esterase and primary antibody (mouse anti-PGE_2) were added. Plates were then incubated at room temperature overnight, reaction mixtures were removed, and wells were washed with 10 mM potassium phosphate buffer containing 0.05% Tween 20. Ellman's reagent (200 μL) was added to each well and the plate was incubated at room temperature (exclusion of light) for 60 min, until the control wells yielded an OD = 0.3–0.8 at 412 nm. A standard curve with PGE_2 was generated from the same plate, which was used to quantify the PGE_2 levels produced in the presence of test samples. Results were expressed as a percentage relative to a control (solvent-treated samples). All determinations were performed in duplicate, and values generally agreed within 10%. Dose–response curves were generated for the calculation of IC_{50} values.

4.2. Electromechanical studies on smooth muscle preparations

Guinea pigs of both sexes (340–480 g) were killed with a blow on the neck. After excision of the heart the aorta and the ileum were dissected. The aorta was stored at room temperature in gassed (95% O_2–5% CO_2), modified Krebs–Henseleit solution with the following composition (in mmol/L): NaCl 118.0, KCl 4.7, $CaCl_2$ 1.8, $MgSO_4$ 5.8, KH_2PO_4 1.4, $NaHCO_3$ 11.9, and glucose 10. The aorta was cleaned of loosely adhering fat and connective tissue and cut into rings of 2 mm width. Aortic rings were precontracted with 90 mmol/L KCl.

The terminal portion of the ileum was removed and the 10 cm nearest to the caecum was discarded. The intestine was placed in a nutrient solution. The intestine was cleaned by flushing with nutrient solution and cut into pieces of 1–2 cm length.

The arteria pulmonalis was dissected close to the heart, cleaned, and cut into rings of 2 mm width. After the isolation the preparations (terminal ilea, aortic, and arteria pulmonalis rings) were stored at room temperature in gassed (95% O_2–5% CO_2) Krebs–Henseleit solution with the following composition (in mmol/L): NaCl 114.9, KCl 4.73, $CaCl_2$ 3.2, $MgSO_4$ 1.18, $NaHCO_3$ 24.9, KH_2PO_4 1.18, and glucose 10, pH 7.2–7.4.

Isometric contraction force of terminal ilea precontracted by 60 mmol/L KCl, aortic and arteria pulmonalis rings precontracted by 90 mmol/L KCl was measured by the method described by Reiter.[45] The preparations were placed in a continuously oxygenated

(95% O_2 and 5% CO_2) bath of 28 mL nutrient solution to guarantee sufficient oxygen supply and appropriate pH as well as circulation of nutrient solution with and without test compound. The experiments were performed at a temperature of 37 ± 1 °C. The smooth muscle preparations were connected with one end to a tissue holder and the other to a force transducer (Transbridge™, 4-Channel Transducer Amplifier, World Precision Instruments, Sarasota, FL, USA). Resting tension of 19.6 mN (aortic rings), 4.9 mN (terminal ileum) or 9.8 mN (arteria pulmonalis rings) was kept constant throughout the experiments.

After a control period of 45 min the different concentrations of the compounds were added to the bathing solution cumulatively, until a steady state was reached.

Signals were recorded with a chart recorder (BD 112 Dual Channel, Kipp & Zonen) and evaluated. For statistical analyses the arithmetic means and standard error of the mean (SEM) of n experiments were calculated. Statistical significance of the results was evaluated by Student's *t* test for paired observations.

Due to insolubility of the test compounds in aqueous nutrient solution, stock solutions of the compounds **3**, **4**, and **9**–**11** were dissolved in dimethylsulfoxide (DMSO) every day and were further diluted with modified Krebs–Henseleit solution to the required concentrations. To exclude the DMSO effect, a series of experiments with DMSO only was performed at the same experimental conditions. The DMSO effect was subtracted from the results of the compounds.

4.3. Chemistry

All chemicals obtained from commercial suppliers were used as received and were of analytical grade. Melting points were determined on a Kofler hot stage apparatus and are uncorrected. The ^1H and ^{13}C NMR spectra were recorded on a Bruker Avance DPx200 (200 and 50 MHz). Chemical shifts are reported in δ values (ppm) relative to Me_4Si line as internal standard and *J* values are reported in Hertz. Mass spectra were obtained by a Hewlett Packard (GC: 5890; MS: 5970) spectrometer. Solutions in organic solvents were dried over anhydrous sodium sulfate.

4.3.1. 3-Bromo-1,2-dihydronaphthalene (1). 3-Bromo-1,2-dihydronaphthalene (**1**) was synthesized as reported by Napolitano et al.[46]

4.3.2. 3-Bromo-1,2-dihydro-7-methoxynaphthalene (2). 3-Bromo-1,2-dihydro-7-methoxynaphthalene (**2**) was synthesized as reported by Bhattacharya et al.[47]

4.3.3. General procedure for synthesis of compounds 3–7 and 9–11. General procedure for synthesis of compounds **3**–**7** and **9**–**11**: In a 50-ml three-necked flask the brominated 1,2-dihydronaphthalene or 1*H*-indene (2 mmol) was mixed with the corresponding phenyl boronic acid (2.2 mmol), potassium carbonate (0.552 g, 4 mmol, 2.0 M solution in water), 12 mL toluene, and 0.8 mL ethanol. The suspension was stirred under argon for 30 min at room temperature. Then tetrakis(triphenylphosphine)palladium(0) (0.068 g, 0.06 mmol) with 0.6 mL ethanol was added and the mixture was heated to 90 °C under argon. After cooling to room temperature the mixture was extracted with 5% $NaHCO_3$ solution, saturated $NaHCO_3$ solution, saturated brine, and water several times, then the organic layer was dried over anhydrous sodium sulfate and the solvent was removed under reduced pressure. The raw products were recrystallized to yield compounds **3**–**7** and **9**–**11**, respectively.

4.3.4. 1,2-Dihydro-3-(2,3,4-trimethoxyphenyl)naphthalene (3). 1,2-Dihydro-3-(2,3,4-trimethoxyphenyl)naphthalene (**3**) was synthesized from 3-bromo-1,2-dihydronaphthalene (**1**) (0.416 g, 2 mmol) and 2,3,4-trimethoxyphenyl boronic acid (0.466 g, 2.2 mmol). The raw product was recrystallized from methanol. Yield: 0.315 g (53%); mp 105–107 °C; ^1H NMR ($CDCl_3$): δ 2.60–2.75 (m, 2H), 2.83–2.97 (m, 2H), 3.83 (s, 3H), 3.88 (s, 3H), 3.90 (s, 3H), 6.56–6.72 (m, 2H), 6.95–7.21 (m, 5H); ^{13}C NMR ($CDCl_3$): δ 28.1, 28.5, 56.0, 61.0, 107.2, 123.0, 125.9, 126.2, 126.5, 126.7, 127.2, 129.7, 134.8, 134.9, 138.4, 142.5, 151.6, 153.1; MS: *m*/*z* 83 (49%), 117 (22%), 125 (20%), 166 (14%), 181 (20%), 296 (M^+, 100%). Anal. calcd for $C_{19}H_{20}O_3 \cdot 0.2$ mol H_2O: C, 76.08; H, 6.85. Found: C, 75.91; H, 6.80.

4.3.5. 1,2-Dihydro-3-(3,4-dimethoxyphenyl)naphthalene (4). 1,2-Dihydro-3-(3,4-dimethoxyphenyl)naphthalene (**4**) was synthesized from 3-bromo-1,2-dihydronaphthalene (**1**) (0.416 g, 2 mmol) and 3,4-dimethoxyphenyl boronic acid (0.400 g, 2.2 mmol). The raw product was recrystallized from ethanol. Yield: 0.142 g (26%); mp 74–76 °C; ^1H NMR ($CDCl_3$): δ 2.63–2.80 (m, 2H), 2.85–3.00 (m, 2H), 3.90 (s, 3H), 3.94 (s, 3H), 6.73–6.92 (m, 2H), 7.03–7.23 (m, 6H); ^{13}C NMR ($CDCl_3$): δ 26.4, 28.2, 55.8, 55.9, 108.3, 111.0, 117.7, 122.9, 126.3, 126.6, 126.7, 127.1, 134.0, 134.6, 134.8, 138.3, 148.6, 148.8; MS: *m*/*z* 43 (22%), 101 (34%), 202 (24%), 215 (100%), 230 (30%), 248 (20%), 266 (M^+, 7%). Anal. calcd for $C_{18}H_{18}O_2$: C, 80.36; H, 6.86. Found: C, 80.33; H, 6.78.

4.3.6. 5-(1,2-Dihydro-3-naphthalenyl)-1,3-benzodioxole (5). 5-(1,2-Dihydro-3-naphthalenyl)-1,3-benzodioxole (**5**) was synthesized from 3-bromo-1,2-dihydronaphthalene (**1**) (0.416 g, 2 mmol) and 3,4-methylenedioxyphenyl boronic acid (0.365, 2.2 mmol). The raw product was recrystallized from ethanol. Yield: 0.210 g (42%); mp 85–90 °C; ^1H NMR ($CDCl_3$): δ 2.59–2.75 (m, 2H), 2.85–3.00 (m, 2H), 5.96 (s, 2H), 6.68–6.85 (m, 2H), 6.97–7.18 (m, 6H); ^{13}C NMR ($CDCl_3$): δ 27.0, 28.6, 101.5, 106.1, 108.6, 119.2, 123.7, 126.8, 127.0, 127.2, 127.6, 135.0, 135.2, 136.0, 138.7, 147.4, 148.3; MS: *m*/*z* 82 (35%), 94 (47%), 124 (23%), 135 (59%), 189 (23%), 219 (16%), 250 (M^+, 100%). Anal. calcd for $C_{17}H_{14}O_2 \cdot 0.4$ mol H_2O: C, 79.29; H, 5.97. Found: C, 79.29; H, 5.79.

4.3.7. 1,2-Dihydro-3-(3,4-dimethoxyphenyl)-7-methoxynaphthalene (6). 1,2-Dihydro-3-(3,4-dimethoxyphenyl)-7-methoxynaphthalene (**6**) was synthesized from 3-bromo-1,2

dihydro-7-methoxynaphthalene (**2**) (0.478 g, 2 mmol) and 3,4-dimethoxyphenyl boronic acid (0.400 g, 2.2 mmol). The raw product was recrystallized from ethanol. Yield: 0.222 g (37%); mp 123–125 °C; ^{1}H NMR ($CDCl_3$): δ 2.64–2.75 (m, 2 H), 2.85–2.98 (m, 2H), 3.81 (s, 3H), 3.90 (s, 3H), 3.94 (s, 3H), 6.66–6.78 (m, 3H), 6.80–6.90 (m, 1H), 7.00–7.12 (m, 3H); ^{13}C NMR ($CDCl_3$): δ 26.2, 28.7, 55.3, 55.8, 55.9, 108.2, 111.0, 111.3, 113.4, 117.4, 122.4, 127.4, 128.0, 134.3, 135.7, 136.3, 148.4, 148.8, 158.5; MS: *m/z* 107 (22%), 115 (28%), 151 (27%), 165 (28%), 281 (31%), 296 (M^+, 100%). Anal. calcd for $C_{19}H_{20}O_3$: C, 77.00; H, 6.80. Found: C, 76.72; H, 6.69.

4.3.8. 1,2-Dihydro-7-methoxy-3-(2,3,4-trimethoxyphenyl)-naphthalene (7). 1,2-Dihydro-7-methoxy-3-(2,3,4-trimethoxyphenyl)naphthalene (**7**) was synthesized from 3-bromo-1,2-dihydro-7-methoxynaphthalene (**2**) (0.478 g, 2 mmol) and 2,3,4-trimethoxyphenyl boronic acid (0.466 g, 2.2 mmol). The raw product was recrystallized from ethanol. Yield: 0.215 g (33%); mp 105–108 °C; ^{1}H NMR ($CDCl_3$): δ 2.62–2.70 (m, 2H) 2.85–2.94 (m, 2H), 3.81 (s, 3H), 3.83 (s, 3H), 3.87 (s, 3H), 3.90 (s, 3H), 6.51–6.75 (m, 4H), 6.92–7.08 (m, 2H); ^{13}C NMR ($CDCl_3$): δ 27.9, 29.0, 55.3, 56.0, 60.9, 61.0, 107.2, 111.2, 113.4, 123.0, 125.3, 127.2, 128.1, 129.9, 135.7, 136.7, 142.5, 151.5, 152.9, 158.5; MS: *m/z* 98 (31%), 148 (20%), 181 (25%), 271 (26%), 326 (M^+, 100%). Anal. calcd for $C_{20}H_{22}O_4$: C, 73.60; H, 6.79. Found: C, 73.32; H, 6.80.

4.3.9. 2-Bromo-1*H*-indene (8). 2-Bromo-1*H*-indene (**8**) was synthesized as reported by Mc Ewen et al.[48]

4.3.10. 5-(2-1*H*-Indenyl)-1,3-benzodioxole (9). 5-(2-1*H*-Indenyl)-1,3-benzodioxole (**9**) was synthesized from 2-bromo-1*H*-indene (**8**) (0.390 g, 2 mmol) and 3,4-methylenedioxyphenyl boronic acid (0.365, 2.2 mmol). The raw product was recrystallized from ethanol. Yield: 0.295 g (62%); mp 151–153 °C; ^{1}H NMR ($CDCl_3$): δ 3.71 (s, 2H), 5.96 (s, 2H), 6.74–6.86 (m, 1H), 7.02–7.46 (m, 7H); ^{13}C NMR ($CDCl_3$): δ 39.2, 101.1, 105.9, 108.4, 119.4, 120.7, 123.5, 124.5, 125.2, 126.6, 130.5, 143.0, 145.4, 146.1, 147.1, 148.0; MS: *m/z* 76 (37%), 89 (36%), 118 (43%), 178 (28%), 205 (19%), 236 (M^+, 100%). Anal. calcd for $C_{16}H_{12}O_2 \cdot 0.1$ mol H_2O: C, 80.72; H, 5.17. Found: C, 80.50; H, 5.04.

4.3.11. 2-(2-Methoxyphenyl)-1*H*-indene (10). 2-(2-Methoxyphenyl)-1*H*-indene (**10**) was synthesized from 2-bromo-1*H*-indene (**8**) (0.390 g, 2 mmol) and 2-methoxyphenyl boronic acid (0.330 g, 2.2 mmol). The raw product was recrystallized from ethanol. Yield: 0.185 g (42%); mp 69 °C; ^{1}H NMR ($CDCl_3$): δ 3.86 (s, 2H), 3.94 (s, 3H), 6.89–7.05 (m, 2H), 7.10–7.31 (m, 3H), 7.34–7.57 (m, 4H); ^{13}C NMR ($CDCl_3$): δ 40.9, 55.3, 111.2, 120.6, 121.0, 123.3, 124.5, 125.2, 126.4, 128.3, 128.6, 130.6, 142.9, 143.1, 145.9, 157.5; MS: *m/z* 76 (57%), 89 (86%), 107 (66%), 119 (36%), 178 (100%), 207 (39%), 222 (M^+, 73%). Anal. calcd for $C_{18}H_{18}O_3$: C, 76.57; H, 6.43. Found: C, 76.30; H, 6.47.

4.3.12. 2-(2,3,4-Trimethoxyphenyl)-1*H*-indene (11). 2-(2,3,4-Trimethoxyphenyl)-1*H*-indene (**11**) was synthesized from 2-bromo-1*H*-indene (**8**) (0.390 g, 2 mmol) and 2,3,4-trimethoxyphenyl boronic acid (0.466 g, 2.2 mmol). The raw product was recrystallized from ethanol. Yield: 0.240 g (42%); mp 107–110 °C; ^{1}H NMR ($CDCl_3$): δ 3.81 (s, 2H), 3.88 (s, 3H), 3.90 (s, 3H), 3.92 (s, 3H), 6.69 (d, J = 8.8 Hz, 1H), 7.08-7.30 (m, 3H), 7.32–7.50 (m, 3H);^{13}C NMR ($CDCl_3$): δ 41.2, 56.4, 60.8, 61.3, 107.9, 121.2, 123.4, 123.7, 123.8, 124.8, 126.9, 129.2, 143.2, 143.3, 146.4, 152.7, 153.6; MS: *m/z* 115 (25%), 153 (50%), 251 (21%), 267 (23%), 282 (100%). Anal. calcd for $C_{16}H_{14}O$: C, 86.45; H, 6.35. Found: C, 86.16; H, 6.28.

4.4. Computational details

Simulations were performed on a series of 8 ligands synthesized by our group. These ligands were designed as bridged resveratrol analogues.

Crystal structures from the Brookhaven Protein Database were taken and provided Cartesian coordinates for murine COX-2 complexed with SC-558 (**1cx2**).[49] Hydrogen atoms were taken from file. Histidin proteins were modeled to represent a pH of 6.5. Hydrogens were added optimizing H-bond network.

The coordinates for COX-1 complexed with flurbiprofen were taken from **1prh**[50] of the Brookhaven Protein Database. Missing hydrogens where added using MolProbity.[51]

The resulting structures were energy minimized using the OPLS-AA[52] force field and a distance-dependent dielectric constant of 4*r*. The protein backbone atoms at this point were kept fixed. All other atoms were allowed to relax to reduce intramolecular strain.

References and notes

1. Jang, M.; Cai, L.; Udeani, G. O.; Slowing, K. V.; Thomas, C. F.; Beecher, C. W.; Fong, H. H.; Farnswoth, N. R.; Kinghorn, A. D.; Mehta, R. G.; Moon, R. C.; Pezzuto, J. M. *Science* **1997**, *275*, 218.
2. Pace-Asciak, C. R.; Hahn, S.; Diamandis, E. P.; Soleas, G.; Goldberg, D. *Clin. Chem. Acta* **1995**, *235*, 207.
3. Kimura, Y.; Okuda, H.; Arichi, S. *Biochim. Biophys. Acta* **1985**, *834*, 275.
4. Belguendouz, L.; Fremont, L.; Gozzelino, M. T. *Biochem. Pharmacol.* **1998**, *55*, 811.
5. Frankel, E. N.; Waterhouse, A. L.; Kinsella, J. E. *Lancet* **1993**, *341*, 1103.
6. Likhitwitayawuid, K.; Sawasdee, K.; Kirtikara, K. *Planta Med.* **2002**, *68*, 841.
7. Samuelsson, B. *J. Am. Chem. Soc.* **1965**, *87*, 3011.
8. Hamberg, M.; Samuelsson, B. *Proc. Natl. Acad. Sci. U.S.A.* **1975**, *72*, 2994.
9. Hamberg, M.; Svensson, J.; Wakabayashi, T.; Samuelsson, B. *Proc. Natl. Acad. Sci. U.S.A.* **1974**, *71*, 345.
10. Bunting, S.; Gryglewski, R.; Moncada, S.; Vane, J. R. *Prostaglandins* **1976**, *12*, 897.
11. Moncada, S.; Gryglewski, R.; Bunting, S.; Vane, J. R. *Nature* **1976**, *263*, 663.
12. Patrono, C. N. *Engl. J. Med.* **1994**, *330*, 1287.
13. Patrono, C. N.; Coller, B.; Dalen, J. E.; FitzGerald, G. A.; Fuster, V.; Gent, M.; Hirsh, J.; Roth, G. *Chest* **2001**, *119*, 39S.

14. Bunting, S.; Moncada, S.; Vane, J. R. *Br. Med. Bull.* **1983**, *39*, 271.
15. Vane, J. R. *Nature* **1971**, *231*, 232.
16. Kitamura, T.; Itoh, M.; Noda, T.; Matsuura, M.; Wakabayashi, K. *Int. J. Cancer* **2004**, *109*, 576.
17. Rotondo, S.; Krauze-Brzosko, K.; Manarini, S.; Evangelista, V.; Cerletti, C. *Eur. J. Pharmacol.* **2004**, *488*, 79.
18. Bottone, F. G.; Martinez, J. M.; Alsto-Mills, B.; Eling, T. E. *Carcinogenesis* **2004**, *25*(3), 349.
19. Krul, E. S. *U.S. Patent* 2003162824, **2003**; CAN 139: 191440, 2003.
20. Teng, X. W.; Abu-Mellal, A. K. M.; Davies, N. M. *J. Pharm. Sci.* **2003**, *6*, 205.
21. Chulada, P. C.; Thompson, M. B.; Mahler, J. F.; Doyle, C. M.; Gaul, B. W.; Lee, C.; Tiano, H. F.; Morham, S. G.; Smithies, O.; Langenbach, R. *Cancer Res.* **2000**, *60*, 4705.
22. Tiano, H. F.; Loftin, C. D.; Akunda, J.; Lee, C.; Spalding, J.; Sessoms, A.; Dunson, D. B.; Rogan, E. G.; Morham, S. G.; Smart, R. C.; Langenbach, R. *Cancer Res.* **2002**, *62*, 3395.
23. Thin, M. J.; Henley, S. J.; Patrono, C. *J. Natl. Cancer Inst.* **2002**, *94*, 252.
24. Steinhilber, D.; Laufer, S. *Pharm. Unserer Zeit* **2004**, *33*, 500.
25. Pettit, G. R.; Grealish, M. P.; Jung, M. K.; Hamel, E.; Pettit, R. K.; Chapuis, J. C.; Schmidt, J. M. *J. Med. Chem.* **2002**, *45*, 2534.
26. Kim, S.; Ko, H.; Park, J. E.; Jung, S.; Lee, S. K.; Chun, Y. J. *J. Med. Chem.* **2002**, *45*, 160.
27. Thakkar, K.; Geahlen, R. L.; Cushman, M. *J. Med. Chem.* **1993**, *36*, 2950.
28. Murias, M.; Handler, N.; Erker, T.; Pleban, K.; Ecker, G.; Saiko, P.; Szekeres, T.; Jaeger, W. *Bioorg. Med. Chem.* **2004**, *12*, 5571.
29. Chen, C. K.; Pace-Asciak, C. R. *Gen. Pharmacol.* **1996**, *27*, 363.
30. Price, M. L. P.; Jorgensen, W. L. *J. Am. Chem. Soc.* **2000**, *122*, 9455.
31. Price, M. L. P.; Jorgensen, W. L. *Bioorg. Med. Chem. Lett.* **2001**, *11*, 1541.
32. Aquist, J.; Marelius, J. *Comb. Chem. High Throughput Screening* **2001**, *4*, 613.
33. Carlson, H. A.; Jorgensen, W. L. *J. Phys. Chem.* **1995**, *99*, 10667.
34. Wall, I. D.; Leach, A. R.; Salt, D. W.; Ford, M. G.; Essex, J. W. *J. Med. Chem.* **1999**, *42*, 5142.
35. Morris, G. M.; Goodsell, D. S.; Halliday, R. S.; Huey, R.; Hart, W. E.; Belew, R. K.; Olson, A. J. *J. Comput. Chem.* **1998**, *19*, 1639.
36. Kuntz, I. D.; Blaney, J. M.; Oatley, S. J.; Langridge, R.; Ferrin, T. E. *J. Mol. Biol.* **1982**, 269.
37. Shoichet, B. K.; Bodian, D. L.; Kuntz, I. D. *J. Comput. Chem.* **1992**, *13*, 380.
38. Gordon, M. S.; Schmidt, M. W. In *Theory and Applications of Computational Chemistry*; Dykstra, C. E., Frenking, G., Kim, K., Scuseria, G., Eds.; Elsevier: Amsterdam, 2005.
39. Schmidt, M. W.; Baldridge, K. K.; Boatz, J. A.; Elbert, S. T.; Gordon, M. S.; Jensen, J. H.; Koseki, S.; Matsunaga, N.; Nguyen, K. A.; Su, S.; Windus, T. L.; Dupuis, M.; Jr, J. A. M. *J. Comput. Chem.* **1993**, *14*, 1347.
40. Solis, F. J.; Wets, R. J.-B. *Math. Oper. Res.* **1981**, *6*, 19.
41. Lindendahl, E.; Hess, B.; van der Spoel, D. *J. Mol. Model.* **2001**, *7*, 306.
42. Schuettelkopf, A. W.; van Aalten, D. M. F. *Acta Crystallogr., Sect. D: Biol. Crystallogr.* **2004**, *60*, 1355.
43. Berendsen, H. J.; Postma, J. P.; van Gunsteren, W. F.; Hermans, J. *Interaction Models for Water in Relation to Protein Hydration*; D. Reidel Publishing Co.: Dordrecht, 1981.
44. Tounge, B. A.; Reynolds, C. H. *J. Med. Chem.* **2003**, *46*, 2074.
45. Reiter, M. *Arzneim. Forschung* **1967**, *17*, 1249.
46. Napolitano, E.; Fiaschi, R.; Mastrorilli, E. *Synthesis* **1986**, *2*, 122.
47. Bhattacharya, S.; Mandal, A. N.; Chaudhuri, S. R. R.; Chatterjee, A. *Tetrahedron Lett.* **1984**, *25*, 3007.
48. Mc Ewen, I.; Roennquist, M.; Ahlberg, P. *J. Am. Chem. Soc.* **1993**, *115*, 3989.
49. Kurumbail, R. G.; Stevens, A. M.; Gierse, J. K.; McDonald, J. J.; Stegeman, R. A.; Pak, J. Y.; Gildehaus, D.; Miyashiro, J. M.; Penning, T. D.; Seibert, K.; Isakson, P. C.; Stallings, W. C. *Nature (London)* **1996**, *384*, 644.
50. Picot, D.; Loll, P. J.; Garavito, R. M. *Nature (London)* **1994**, *367*, 243.
51. Lovell, S. C.; Davis, I. W.; Arendall, B. W., III; de Bakker, P. I. W.; Word, M. J.; Prisant, M. G.; Richardson, J. S.; Richardson, D. C. *Proteins: Struct. Funct. Genet.* **2003**, *50*, 437.
52. Jorgensen, W. L.; Tirado-Rives, J. *J. Am. Chem. Soc.* **1988**, *110*, 1657.